Eur Biophys J (1997) 26: 359–369

ARTICLE

Anja von Nahmen · Andreas Post
Hans-Joachim Galla · Manfred Sieber

The phase behavior of lipid monolayers containing pulmonary surfactant protein C studied by fluorescence light microscopy

Received: 13 February 1997 / Accepted: 22 May 1997

Abstract Three compounds of the pulmonary surfactant – dipalmitoylphosphatidylcholine (DPPC), dipalmitoylphosphatidylglycerol (DPPG), and the surfactant associated protein C (SP-C) – were spread at the air-water interface of a Langmuir trough as a model system to mimic the properties of natural surfactant. Fluorescence microscopical images of the film formed at the interface were obtained during compression using a fluorescence dye bound covalently either to phosphatidylcholine or to SP-C. The images were quantified using statistical methods in respect to relative areas and relative fluorescence intensities of the domains found. In the early stage of compression, film pressure rose slightly and was accompanied by a phase separation which could be recognized in the images by the formation of bright and dark domains. On further compression, after a steep increase of film pressure, a plateau region of constant film pressure started abruptly. During compression in the plateau region, fluorescence intensity of the bright domain formed in the early stage of compression increased. The increasing fluorescence intensity, the non-Gaussian intensity distribution of the bright domain, and the small mean molecular area of the film in the plateau region gave rise to the assumption that multilayer structures were formed in the late stage of compression. The formation of the multilayer structures was fully reversible in repeated compression-expansion cycles including the plateau region of the phase diagram. The ability of lipid/SP-C mixtures to form reversible multilayer structures during compression may be relevant to stability in lungs during expiration and inhalation.

Key words Pulmonary surfactant · Surfactant protein C · SP-C · Fluorescence light microscopy · Phospholipids · Monolayer · Lipid-protein interactions

A. von Nahmen · A. Post · H.-J. Galla · M. Sieber (✉)
Institut für Biochemie, Westfälische Wilhelms-Universität,
Wilhelm-Klemm-Strasse 2, D-48149 Münster, Germany
(e-mail: sieber@uni-muenster.de; Fax: +2 51-8 33 32 06)

Abbreviations DPPC 1,2-Dipalmitoyl-sn-glycero-3-phosphocholine · DPPG 1,2-Dipalmitoyl-sn-glycero-3-(phospho-rac-(1-glycerol)) · FLM fluorescence light microscopy · NBD fluoride 4-Fluoro-7-nitrobenz-2-oxa-1,3-diazole · NBD-PC 1-Palmitoyl-2-(6-((7-nitro-2-1,3-benzoxadiazol-4-yl)amino)caproyl)-sn-glycero-3-phosphocholine · NBD-SP-C nitrobenzoxadiazol labeled surfactant associated protein C · SP-C surfactant associated protein C · A_b^* relative area of the bright domain · A_b absolute area of the bright domain · A_d^* relative area of the dark domain · A_d, absolute area of the dark domain · A_M molecular area · I_{dye}^* relative intensity per fluorescence dye · $\overline{I_b}$ mean intensity of the bright domain · $\overline{I_d}$ mean intensity of the dark domain · $\overline{\Delta I}$ difference of the mean intensities of the bright and the dark domain ($\overline{\Delta I} = I_b - I_d$) · N_b intensity distribution of the bright domain · N_d intensity distribution of the dark domain · N_t total number of pixels of the analyzed frame

Introduction

Pulmonary surfactant is a surface active material present in the lung of mammals. It is produced by the alveolar type II cells and secreted into the extracellular fluid layer lining the epithelial cells of the alveoli. It is generally accepted that pulmonary surfactant spreads at the air-liquid interface forming a monomolecular film. The presence of the surfactant monolayer is a prerequisite for a proper pulmonary function because it reduces and adapts the surface tension of the interface dynamically to the varying surface area of the alveoli during breathing.

Surfactant obtained by bronchoalveolar fluid lavage is composed of 85–90% lipids, 10% of proteins, and 2% of carbohydrates (King and Clements 1972; Harwood 1987). The main components of the lipid matrix are dipalmitoylphosphatidylcholine (DPPC) and phosphatidylglycerols (PG's). Most of the fatty acid residues of the lipids are saturated (Harwood 1987). There are four surfactant-specific proteins found in the bronchoalveolar fluid called SP-A,

SP-B, SP-C, and SP-D (Johansson et al. 1994). Because of their hydrophobic nature, SP-B and SP-C are assumed to be particularly important in determining the biophysical properties of the surfactant (Oosterlaken-Dijksterhuis et al. 1991; Baatz et al. 1990; Taneva and Keough 1994 a – d).

The most commonly accepted explanation for the dynamic adjustment of the surfactant monolayer area during respiration is the so-called "squeeze-out" hypothesis. According to this theory, non-DPPC compounds are selectively squeezed out of the monolayer into the subphase during compression (expiration). The low surface tension necessary to ensure stable conditions in the lung is established by the nearly pure DPPC monolayer remaining at the air-liquid interface. On expansion (inhalation), the material squeezed out respreads at the surface with the help of the surfactant associated proteins. Recent studies question this theory (Scarpelli and Mautone 1994). Recently, Schürch et al. (1995) provided transmission electron micrographic evidence that the surface film associated with the air-alveolar interface seems to consist of several layers in rat lung thin sections.

In this study, we examined the functional role of the surfactant protein SP-C (reviewed in: Beers and Fisher 1992; Johansson et al. 1994 a) in the dynamic adjustment of surfactant properties in vitro. With a molecular weight of ~4000 Da, SP-C is the smallest of the surfactant-specific proteins. The sequence of 35 amino acids – for the human protein – is characterized by a hydrophobic carboxy-terminal region comprising 23 amino acids (mainly valine, leucine or isoleucine). This extremely hydrophobic part of the molecule is highly conserved between different species. In the case of porcine SP-C, it has been shown by NMR that this part forms an α-helix (Johansson et al. 1994 b; Johansson et al. 1995). The remaining amino-terminal part of the protein consists mainly of hydrophilic amino acids. Two palmitic acids are linked to the protein via two cysteines located in the hydrophilic part. At physiological pH-values, SP-C has a doubly positive net charge due to two basic amino acid residues located at the transition from the hydrophobic to the hydrophilic region of the protein.

It is the aim of this study to show that important properties of natural lung surfactant can be mimicked by a mixture of two lipids – DPPC and dipalmitoylphosphatidylglycerol (DPPG) – and the surfactant protein SP-C. The phase behavior of the lipid-protein mixture spread at the air-water interface was investigated by means of surface balance studies. Additionally, fluorescence light microscopy (FLM) was used to visualize the structures formed at the interface during compression of the spread film.

Materials and methods

Materials

1,2-Dipalmitoyl-sn-glycero-3-phosphocholine (DPPC) and 1,2-Dipalmitoyl-sn-glycero-3-(phospho-rac-(1-glycerol)) (DPPG) were obtained from Avanti Polar Lipids Inc. (Alabaster, AL, USA) and were used without further purification. 1-Palmitoyl-2-(6-((7-nitro-2-1,3-benzoxadiazol-4-yl)amino)caproyl)-sn-glycero-3-phosphocholine (NBD-PC) and 4-fluoro-7-nitrobenz-2-oxa-1,3-diazole (NBD fluoride) were purchased from Molecular Probes (Eugene, OR, USA). A dipalmitoylated form of the human recombinant surfactant protein C (SP-C) with the sequence GIPCCPVHLKRLLIVVVVVVLIVVVIVGALLMGL was a generous gift from Byk-Gulden Pharmaceuticals (Konstanz, FRG). After purification of the protein by chromatographic methods, the identity was checked by matrix assisted laser desorption ionization mass spectrometry (MALDI-MS). A molecular mass of 4025 Da confirmed the given primary structure. All solvents were HPLC grade and obtained from Merck (Darmstadt, FRG).

Synthesis of NBD labeled SP-C

The synthesis is based on earlier investigations on the reactivity of NBD fluoride with amines and proteins (Miyano et al. 1985; Toyo'oka et al. 1983). The protein was dissolved in $CHCl_3/CH_3OH$ (1 : 1, v : v). After addition of a 30 fold molar excess of NBD fluoride in CH_3CN the solution was vortexed for 30 min at a temperature of 40 °C. The NBD labeled protein was separated from the educts via reversed phase HPLC using the column Grom Sil C4 (Grom, FRG). The probe was eluted with a linear gradient of H_2O (0.1% TFA)/$CH_3CHOHCH_3$ (0.1% TFA). Matrix assisted laser desorption ionization mass spectrometry was applied to determine the amount of labeled amino acid residues. The mass spectrum showed two peaks corresponding to mono- and di-labeled protein. For all experiments carried out with labeled proteins, the mixture of the two species was used.

Film balance measurements

Film balance experiments were performed on an analytical Wilhelmy-balance (Riegler and Kirstein, Mainz, FRG) with an operation area of 144 cm^2. All surface pressure-area measurements were performed at a temperature of 20 °C on a pure water subphase (purified with a Milli-Q_{185} Plus system, Millipore GmbH, Eschborn, FRG). Monolayers were prepared by spreading aliquots of lipid/SP-C mixtures directly from a $CHCl_3/CH_3OH$ (1 : 1, vol : vol) solution onto the surface. The solvents were allowed to evaporate for 10 min. Compression was then started at a rate of 0.03 nm^2 per molecule per minute. The composition of the investigated films was either DPPC/DPPG (molar ratio 4 : 1) or DPPC/DPPG with 0.4 mole% SP-C.

Fluorescence light microscopy (FLM) of surface films

The fluorescence of the monolayer was excited and visualized by an epifluorescence microscope (Olympus STM5-

MJS, Hamburg, FRG). The trough of the film balance was placed on a specially designed stage (Riegler and Kirstein, Mainz, FRG) for the microscope. With the help of the remote controlled stage, the trough could be moved independently in the three directions of the axes (x, y, z) of a Cartesian coordinate system where the x and y axes were oriented perpendicular to the optical axis of the objective lens. For excitation, a high-pressure mercury lamp with a power of 50 Watt was used. Discrimination of excitation light and emitted light of the probe molecules was achieved by cut-off filters. Images of the monolayer were taken with a CCD camera (Proxicam, Proxitronic, FRG) and stored with a conventional video tape recorder.

Visualization by FLM was made possible either by addition of a fluorescence labeled phosphatidylcholine (NBD-PC, 1 mole% with respect to all lipid), or the labeled protein (NBD-SP-C). Apart from the probe molecules, the composition of the film was the same as described above. Despite of the fact that the addition of NBD-PC has an influence on the isotherms of pure lipids (Leufgen et al. 1996), no significant changes of the isotherms of the lipid/protein mixtures were observed on introduction of one of the probes.

Semi-quantitative evaluation of the images obtained by fluorescence microscopy

The frames stored on a video tape recorder during the measurements were converted to digital images using a frame grabber interface for IBM personal computers. One image consists of 640 times 512 pixels. The value of the intensity of each pixel was encoded as an integer between 0 and 127. Care was taken to keep a constant gain during the experiments.

Owing to the inhomogeneous illumination of the monolayer by the light source, only a part of the original images (total number of pixels, $N_t \sim 10^6$) was used for further analysis. In addition, the intensities of the pixels $I_{xy,raw}$ in the remaining area of the image were corrected. This was done by fitting a paraboloid to the raw image data and subtracting the paraboloid from the data. The corrected values of the intensities of the pixel $I_{x,y}$ at the locations x, y are given by

$$I_{xy} = I_{xy,raw} - M_x(x - x_0)^2 - M_y(y - y_0)^2 \qquad (1)$$

where $I_{xy,raw}$ are the raw values, and M_x, M_y, x_0, y_0 are fitted parameters characterizing the inhomogeneous illumination of the monolayer. This procedure is similar but more specific to 2-dimensional low pass filtering of the data because the typical illumination profile of the light source is taken into account.

Results

Film balance experiments were performed using a 4 : 1 molar ratio mixture of the neutral phospholipid dipalmitoylphosphatidylcholine and the charged dipalmitoylphosphatidylglycerol, representing the ratio of neutral and negatively charged lipids found in human lung lavages (Harwood, 1987). In the case of protein/lipid films, the protein content was set to 0.4 mole% in accordance with earlier investigations (Post et al. 1995) and the fact that in lung lavages the content of hydrophobic proteins was found to be less than one percent (Curstedt et al. 1987).

Upon compression, the DPPC/DPPG monolayer showed the typical behavior of complex lipid mixtures in the region of low film pressures (Fig. 1 a): after reaching a mean molecular area A_M of about 0.7 nm^2, the film pressure π rose continuously. In the region of steepest film pressure increase (lowest compressibility) the molecular area was about 0.45 nm^2 which matches with the molecular area of a pure DPPC monolayer in the solid state. On further compression, the isotherm exhibited a brief plateau followed by continued pressure increase. Up to a pressure of about 60 mN/m all processes proved to be fully reversible. This is shown by two successive compression/expansion cycles, where no significant shift of the isotherms can be observed.

On compression, the spread lipid/SP-C mixture showed, in the region of low film pressures, the same behavior as

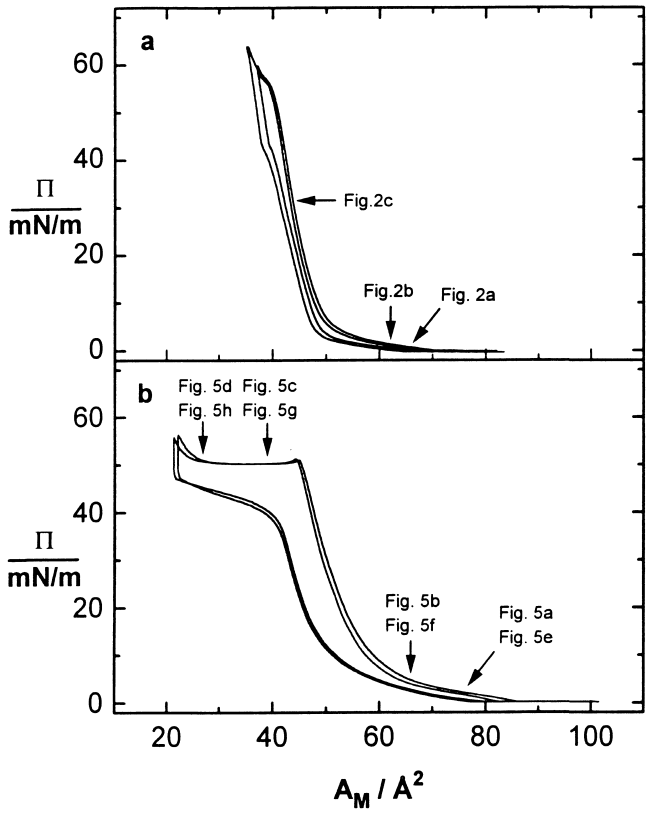

Fig. 1 Compression/expansion cycles of mixed phospholipid (**a** DPPC/DPPG, molar ratio 4 : 1) and phospholipid/SP-C (**b** DPPC/DPPG/SP-C, lipid molar ratio 4 : 1, protein content 0.4 mole%) films. The complete first and second cycle is shown. The compression/expansion rate was 3 Å^2 per molecule and minute. The *arrows* denote the state of the films, at which the different fluorescence images shown in Fig. 2, and Fig. 5, were taken

described for the lipid monolayer: after reaching a mean molecular area A_M of about 0.8 nm^2, the film pressure π increased continuously to a value of 50 to 55 mN/m (Fig. 1 b). At such pressures, the mean molecular area A_M is at a maximum 0.45 nm^2. On further compression, the compressibility of the lipid/protein film increased abruptly. This became apparent in the surface pressure area diagram as a distinct plateau region. The transition from the region of steep increase in film pressure to the plateau region was sharply defined. The end of the plateau region was characterized by a further increase of film pressure. The mean molecular area defining this increase at the end of the plateau region varied strongly depending on the compression speed. Under the conditions described above, film pressure increased at a molecular area of about 0.25 nm^2. Repeated compression-expansion cycles including the plateau region led to no significant change of the isotherms. Slight shifts to lower molecular areas were due to reorientation processes in the film during the period of the experiment.

Fluorescence light microscopic investigations of both films of the lipid mixture and the lipid/protein mixture showed that the films undergo a phase separation at low pressures. This became apparent by the appearance of two kinds of domains distinguishable by the intensity of fluorescence light emitted by the dyes. Dark domains always appeared in the form of round patches of varying size (Figs. 2 and 5). Nag et al. (1991) previously showed that the distribution of domain size in monolayers of DPPC depends on the compression rate, but that this distribution does not effect the percentage of the total area occupied by the dark domains. This observation was confirmed in this study.

In order to calculate the areas A_d and A_b of the surface covered by the domains, the dark domains (d) and the bright domain (b), and the mean fluorescence intensities per area, $\overline{I_d}$ and $\overline{I_b}$, histograms of the fluorescence intensities were analyzed from digitalized images. The histograms could be fitted in most cases by a sum of two Gaussian's as shown in Fig. 2. Each of the Gaussian's represents the intensity distribution of the dark domains $N_d(I)$ or the bright domain $N_b(I)$. The parameters A_d, A_b, $\overline{I_d}$, and $\overline{I_b}$ were calculated from the integral and the mean of the Gaussian's:

$$\frac{N(I)}{N_t} = \frac{1 - A_b^*}{\sigma_d \sqrt{\pi}} \exp\left\{\frac{-(I - \overline{I_d})^2}{\sigma_d^2}\right\} + \frac{A_b^*}{\sigma_b \sqrt{\pi}} \exp\left\{\frac{-(I - \overline{I_b})^2}{\sigma_b^2}\right\} \quad (2)$$

$N(I)$ is the number of pixels with the intensity I, N_t the total number of pixels, $A_d^* = A_d/(A_d + A_b)$ and $A_b^* = A_b/(A_d + A_b)$ are the relative areas ($0 < A^* < 1$) of the dark and the bright domains, and $\overline{I_d}$ and $\overline{I_b}$ are the corresponding mean intensities. The parameters σ_d and σ_b represent the width of the distributions. The usually low signal-to-noise ratio accompanied of fluorescence light microscopy on monolayers, the inhomogeneous illumination of the film by the light source, and the inhomogeneous distribution of the fluorescence dye within the domains contribute to the parameter σ. Therefore, a further analysis of σ during changes of state was omitted. All data sets presented below result from two independent measurements. The errors estimated by the fitting procedure were less than 5% for determination of the relative areas and less than 1% for the mean intensities. The errors are much smaller than the variations from one image to another.

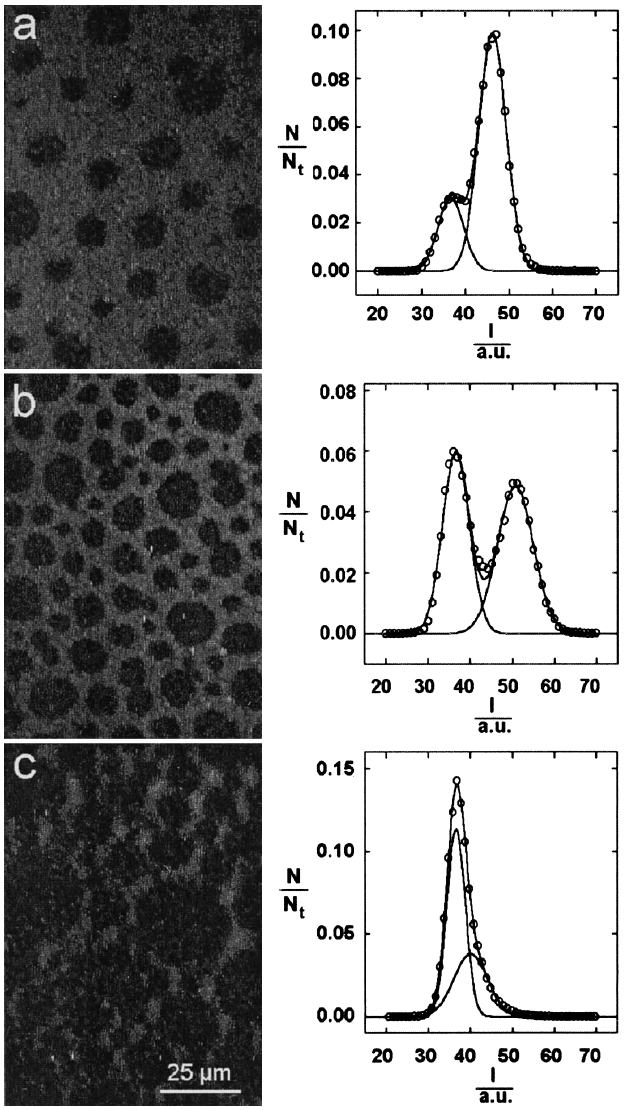

Fig. 2 Typical fluorescence images of a DPPC/DPPG monolayer (molar ratio 4 : 1, dye: NBD-PC, 1 mole% of lipid) taken at different stages of compression (**a** $A_M = 0.66$ nm^2, **b** $A_M = 0.62$ nm^2, **c** $A_M = 0.44$ nm^2). The histograms show the ratio of the number of pixels N with an intensity I to the total number of pixels in the frame N_t. *Circles* represent the data evaluated from the images, whereas the lines were calculated by fitting the sum of two Gaussians. Both, the sum and the individual Gaussians belonging to the dark and the bright domains were drawn

When using lipid films consisting of a mixture of DPPC, DPPG, and the fluorescence dye NBD-PC, domain formation was observed in the early stage of compression. The domains characterized by a low fluorescence intensity ap-

peared in the form of round patches of varying size. The covering with dark patches as well as the fluorescence intensity of the surrounding bright domain increased during compression until a molecular area of $A_M = 0.55$ nm^2 was reached. On further compression the contrast of the images, i. e. the difference in fluorescence intensity between the domains, vanished. These results were quantified by analyzing the histograms evaluated from the images.

Figure 3 a depicts the course of the relative area of the bright domain A_b^* and Fig. 3 b the difference in fluorescence intensity between the bright and the dark domains $\overline{\Delta I}$ ($\overline{\Delta I} = \overline{I_b} - \overline{I_d}$) during compression. At molecular areas of $0.55\ \text{nm}^2 \leq A_M \leq 0.67\ \text{nm}^2$ $\overline{\Delta I}$ increased while A_b^* decreased. This reflects an enrichment of the dye in the bright domain. Lösche et al. (1984) and McConnel et al. (1984) explained the phenomenon by a less dense packing of the lipids in the bright domain with respect to the dark domain. Since A_b^* decreases during compression, it is reasonable to assume a phase transition from an expanded to a condensed phase in this region of the phase diagram. Apart from the fact that the phase separation of DPPC/DPPG monolayers occurs at higher pressure on a sodium chloride subphase, a similar increase of condensed phase was observed during compression by Nag et al. (1994). At a molecular area of $A_M < 0.55$ nm^2 $\overline{\Delta I}$ decreases with decreasing molecular area. Since the mean intensity and the intensity distribution of the dark domain remains constant, this phenomenon cannot be ascribed to diffusion of the dye into the dark domain but to a self-quenching process. Under these conditions, i. e. low contrast between the domains, data analysis is problematic (Fig. 2 c)[1], and the calculated A_b^* and $\overline{\Delta I}$ show greater variations (Fig. 3 a and b, left side).

Figure 4 depicts the course of the relative fluorescence intensity per dye molecule I_{dye}^* during compression. This quality of the dye molecules can be used as an indicator for the physical state of the lipids. I_{dye}^* can be evaluated by assuming that all dye molecules are solved in the less dense phase. Leufgen et al. (1996) confirmed this by secondary ion mass spectrometry investigations on DPPC monolayer containing NBD-PC. The absence of dyes in the condensed phase (surface concentration $\Gamma_{d,dye} \cong 0$) is also indicated by the fact that the mean fluorescence intensity of the dark domains $\overline{I_d}$ has a constant value at all stages of the experiment. Small fluctuations were due to deviations of the light source intensity. Hence, $\overline{I_d}$ can be understood as a background contribution based on scattered excitation light and offsets of the detection system. Taking this into account, the relative fluorescence intensity per dye I_{dye}^* ($0 \leq I_{dye}^* \leq 1$) was obtained from the experimental data using the expression

$$I_{dye}^* = \frac{1}{C \cdot x_{dye}} \cdot A_b^* \cdot A_M \cdot (\overline{I_b} - \overline{I_d}) \qquad (3)$$

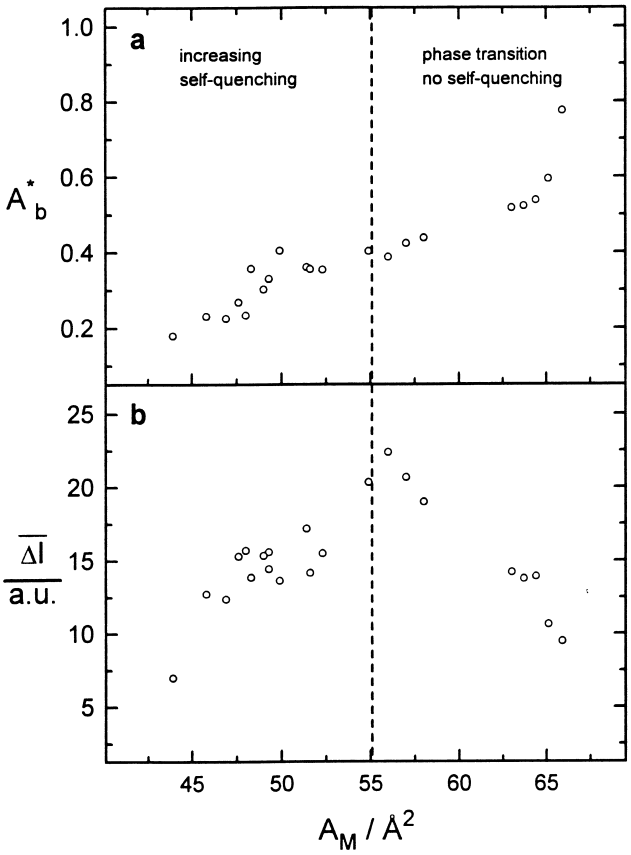

Fig. 3 Dependence of the relative area A_b^* of the bright domains (**a**) and the intensity difference $\overline{\Delta I}$ ($\overline{\Delta I} = \overline{I_b} - \overline{I_d}$) between the bright and the dark domains (**b**) of a lipid (DPPC/DPPG, molar ratio 4 : 1) monolayer on the molecular area A_M. Data were obtained from two independent film preparations

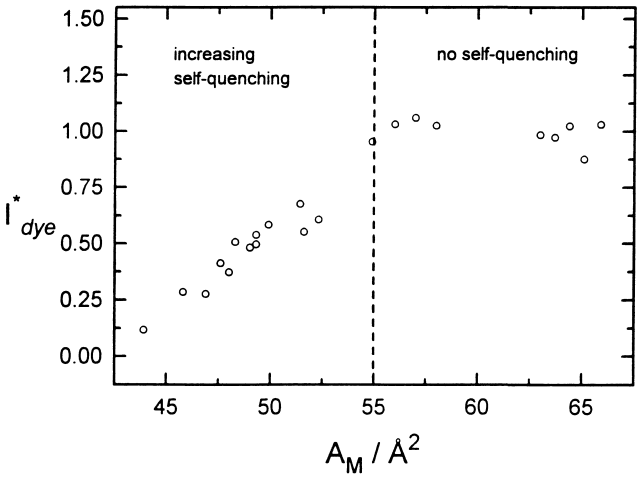

Fig. 4 Relative fluorescence intensity per dye molecule I_{dye}^* in dependence on the molecular area A_M of the lipid (DPPC/DPPG, molar ratio 4 : 1) monolayer. I_{dye}^* was calculated according to Eq. (3). The data are normalized with respect to the fluorescence intensity of the unquenched dye I_{dye}^{∞}. The normalization constant was calculated from the mean of the data with molecular areas larger than 0.55 nm^2 ($I_{dye}^* = 1$)

[1] The intensity distribution of the bright domain is different from a Gaussian distribution at intensity values $I < \overline{I_b}$. Such changes may be due to the self-quenching of the dye and will be the subject of further investigations

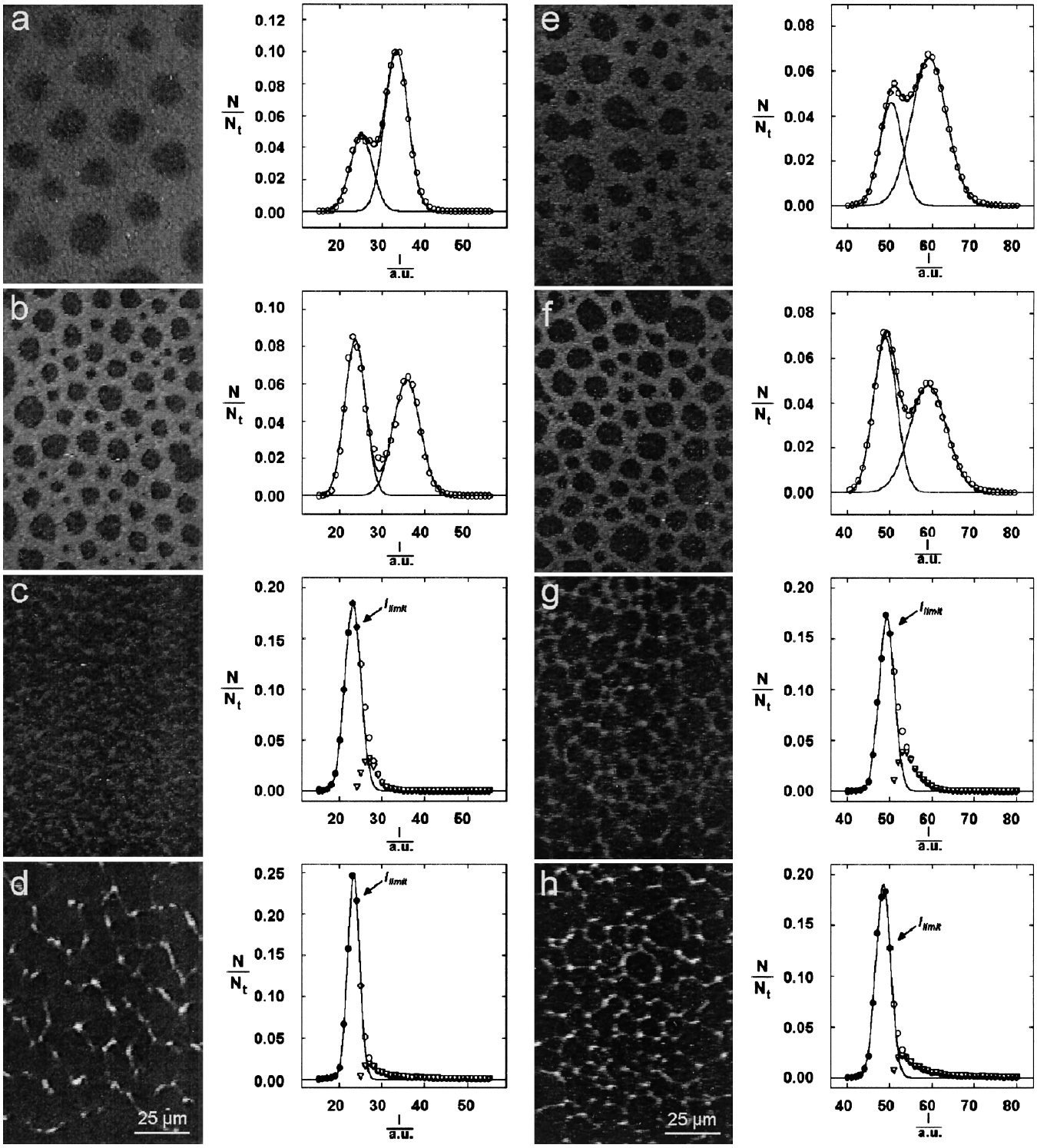

Fig. 5 a–h Typical fluorescence images of a lipid/SP-C film (lipid molar ratio 4 : 1; protein content 0.4 mole%) taken at different stages of compression. Two different fluorescence dyes were used: images **a–d** were taken from films prepared with fluorescence labeled lipid (NBD-PC, 1 mole% in respect to lipid; **a** $A_M = 0.74$ nm^2, **b** $A_M = 0.67$ nm^2, **c** $A_M = 0.39$ nm^2, **d** $A_M = 0.27$ nm^2), and images *e–h* from films prepared with fluorescence labeled protein (NBD-SP-C, 100% labeled; **e** $A_M = 0.75$ nm^2, **f** $A_M = 0.66$ nm^2, **g** $A_M = 0.39$ nm^2, **h** $A_M = 0.27$ nm^2). The histograms show the ratio of the number of pixels N with an intensity I to the total number of pixels in the frame N_t. *Circles* represent the data evaluated from the images. *Lines* in the histograms of the images **a, b, e,** and **f** were calculated as stated in the caption of Fig. 2. *Lines* in the histograms of the images, **c, d, g,** and **h** were calculated by fitting a Gaussian to a part of the intensity distribution of the dark domain (*solid circles*, $I \leq I_{\mathrm{limit}}$). *Triangles* represent the intensity distribution of the bright domain evaluated by subtraction of the Gaussian from the whole distribution

where x_{dye} is the mole fraction of the dye in the spread mixture, and C is an apparatus constant. C was calculated from the fluorescence intensity values obtained at molecular areas of $A_M \geq 0.55$ nm^2. Figure 4 clearly shows that self-quenching occurred only at lower molecular areas (for details see appendix).

The self-quenching can be related to two phenomena: a concentration dependent self-quenching of the dye, as previously reported on the basis of vesicle experiments (Nichols and Pagano 1981; Horowitz et al. 1992), and quenching due to changes of the molecular structure in the film. With increasing surface pressure even the lipids of the former expanded phase are in a condensed state. The self-quenching may then be explained by an increasing alignment of the dyes to each other resulting in strong dipole-dipole interactions.

In the case of the lipid/protein mixture, a similar phase separation was observed in the low surface pressure region of the isotherm (Fig. 5 a, b, e, f). On compression in the collapse region, an increase in contrast, i. e. an increase in fluorescence intensity of the bright domain, was clearly recognizable in the images (Fig. 5 c, d, g, h). This qualitative impression was confirmed by the analysis of the histograms. In contrast to the histograms evaluated from the images taken in the low surface pressure region of the isotherm, the intensity distribution of the bright domain is no longer describable by a Gaussian. Instead, the intensity profile is similar to a Poisson distribution. Deviation from the Gaussian was first observed at the start of the collapse region ($A_M = 0.45$ nm^2). With decreasing molecular area this deviation became more distinct, and a fit of data to Eq. (2) was not possible. In order to determine the parameters $\overline{I_d}$, $\overline{I_b}$, A_d^*, and A_b^*, the histograms were analyzed as follows (see also Figs. 5 and 8): up to a certain fluorescence intensity I_{limit} the histograms were fitted by one Gaussian yielding the parameters $\overline{I_d}$ and A_d^* (and $A_b^* = 1 - A_d^*$). The Gaussian was then subtracted from the histogram resulting in the intensity distribution of the bright domain N_b (Fig. 5). Without knowledge of the concrete distribution function, an evaluation of the parameter $\overline{I_b}$ is then possible according to

$$\overline{I_b} = \frac{\sum\limits_{I > I_{\text{limit}}} N_b I}{\sum\limits_{I > I_{\text{limit}}} N_b} \tag{4}$$

with N_b representing the number of pixels of the bright domains with the fluorescence intensity I. The applicability of the procedure was checked by changing the value of I_{limit} in a narrow range. No significant changes in the desired parameters were obtained.

Inspection of the course of the fluorescence intensity difference $\overline{\Delta I}$ between the two kinds of domains, the expected increase with decreasing molecular area in the plateau region was confirmed (Fig. 6 b). The evaluation of the relative fluorescence intensities per dye molecule according to Eq. (3) shows that the increase is not due to a decreasing self-quenching of the dyes (Fig. 7). In contrast, the relative fluorescence intensity per dye remained con-

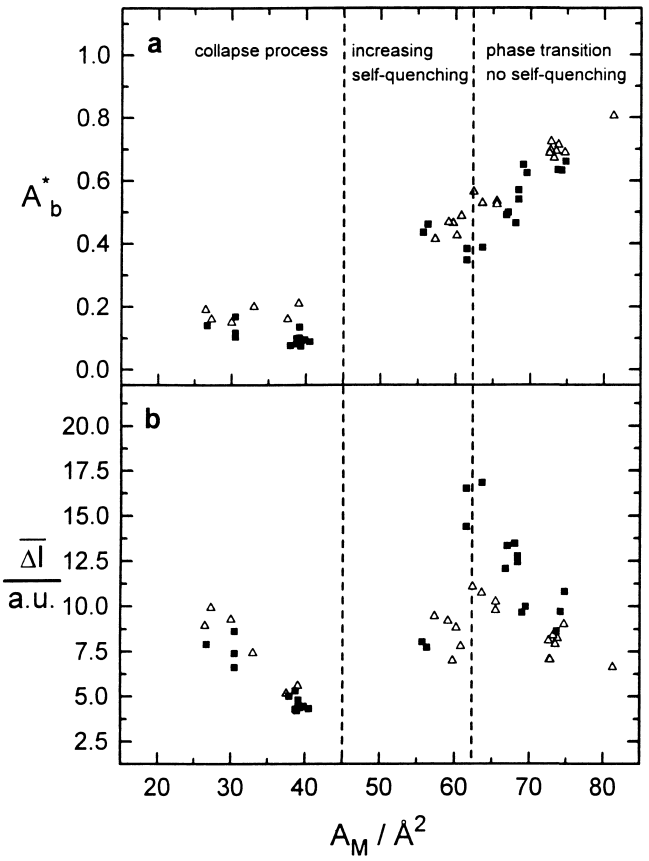

Fig. 6 Dependence of the relative area A_b^* of the bright domains (**a**) and the intensity difference $\overline{\Delta I}$ ($\overline{\Delta I} = \overline{I_b} - \overline{I_d}$) between the bright and the dark domains (**b**) of a lipid/SP-C film (lipid molar ratio 4 : 1; protein content 0.4 mole%) on the molecular area A_M. *Squares* represent data obtained from films prepared with the dye NBD-PC, *triangles* data obtained from films prepared with the dye NBD-SP-C. Each data set was evaluated from two independent film preparations

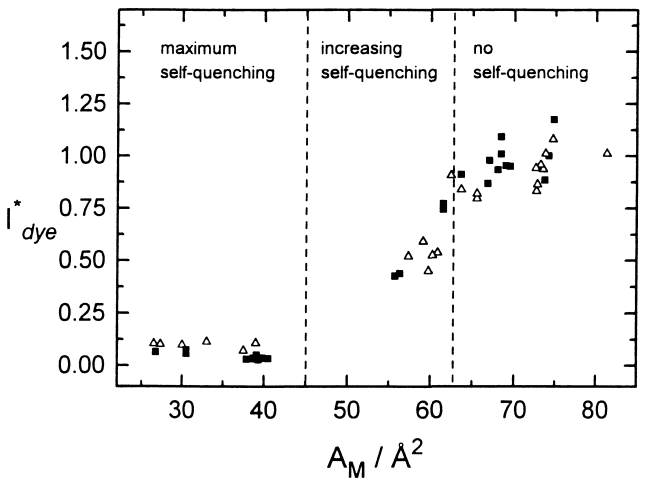

Fig. 7 Relative fluorescence intensity per dye molecule I_{dye}^* in dependence on the molecular area A_M of a lipid/SP-C film (lipid molar ratio 4 : 1; protein content 0.4 mole%). I_{dye}^* was calculated according to Eq. (3). The data are normalized with respect to the fluorescence intensity of the unquenched dye I_{dye}^{∞}. The normalization constant was calculated from the mean of the data with molecular areas larger than 0.65 nm^2 ($I_{dye}^* = 1$)

stant during compression in the collapse region of the phase diagram. Therefore, the increase of $\overline{I_b}$ is due to the increasing surface concentration of the dye molecules, i. e. the decreasing accessible area $A_b^* A_M$.

In contrast to the drop of the relative area A_b^* of the bright domain on compression in the low surface pressure region, it kept constant during compression in the collapse region (Fig. 6), i. e. the area of the bright domains, and the dark domain, respectively, decreased proportionately. Hence, the increase of $\overline{I_b}$ is only due to the decreasing, total surface covered by the film.

Identical observations and analogy were obtained with both the lipid dye NBD-PC and the protein dye NBD-SP-C, indicating that SP-C is always solved in the less dense phase. Differences in the evaluated mean fluorescence intensities were only due to different surface densities of the NBD groups. An enrichment of the protein in the less dense phase was also observed by Nag and coworkers (1996) who used fluorescein labeled SP-C.

Discussion

In this study we examined the behavior of a pulmonary surfactant model system (DPPC/DPPG/SP-C) at the air/water interface of a Langmuir trough. In order to clarify the function of SP-C in this model system, we compared it with a protein free DPPC/DPPG film. Up to a surface pressure of nearly 50 mN/m, the compression characteristics of both films are similar. In contrast to the pure phospholipid film, the lipid/SP-C mixture exhibits a distinct plateau in the phase diagram at a surface pressure of about 50 mN/m. Watkins (1968) and Wang et al. (1995) found a similar plateau at almost the same pressure in phase diagrams of lung lavages of different species. The plateau region extended, as in the model system, over a wide surface area range. This property of the film enables a stable low surface tension at all stages of compression and expansion or, in case of the natural system, at all stages of exhalation and inhalation respectively.

The start of the plateau region is indicated by a spontaneous flattening of the isotherm in the pressure area diagram. Similar shapes of isotherms are observable in studies on pure phospholipids at low surface pressures. In this case, the plateau indicates a phase transition. Our observation can also be understood as a phase transition: a transition of a monolayer phase to a collapse phase stabilized by SP-C. All indications necessary for a phase transition were observed: nearly infinite compressibility at the transition and total reversibility of the process. It has to be pointed out that in the late stage of the transition the mean molecular area A_M falls below the lowest possible value of a pure DPPC monolayer (e.g. $A_{M,DPPC} \approx 0.46$ nm^2). This indicates that the collapse phase is not monomolecular but 3-dimensionally structured.

The fluorescence light microscopic investigations also show the similarity between the surfactant model system and the lipid film in the region of low film pressures. At high molecular areas a phase separation takes place in both systems. From the decrease of the relative area of the bright phase A_b^* and the increase of the fluorescence intensity $\overline{I_b}$ due to the enrichment of the dye molecules, it becomes evident that a liquid expanded phase turns into a liquid condensed phase in this region of the phase diagram. The end of the phase transition is indicated in the phase diagram by a pronounced increase of surface pressure. On further compression beyond this point, all molecules should be in a condensed or even solid state (Albrecht et al. 1978). As described by others (Lösche and Möhwald 1984), an inhomogeneous distribution of the dye is maintained because diffusion is hindered. After the end of the phase transition, a further decrease of the fitted value of A_b^* may be explained by the fact that the strong self-quenching of the dyes leads to a strong overlap of the two intensity distributions which makes the evaluation of all parameters by fitting difficult. Therefore, the area of the surface covered by the former expanded phase may be larger than predicted by the fitted value of A_b^*.

In the case of lipid/SP-C mixtures the condensed phase consists almost exclusively of lipids, as indicated by the low fluorescence intensity in experiments performed in the presence of either the protein or the lipid dye. The protein rich expanded phase exhibits three distinct states dependent on the area available for the film: an expanded state stable in the low surface pressure region of the phase diagram characterized by a high fluorescence intensity, a condensed state present at surface pressures higher than about 10 mN/m, and a collapse state appearing at very high surface pressures of about 50 mN/m. The two latter mentioned states are both characterized by a low fluorescence intensity per dye molecule. In contrast to the condensed state, the fluorescence intensity $\overline{I_b}$ of the phase in the collapse state is increasing on compression. This increase of surface concentration of the dye can be explained by the formation of stacked lipid bilayers. As long as the film is in the collapse state, these bilayer stacks are in contact with the surface active monolayer at all stages of compression and expansion. As depicted in Fig. 8, the formation of multilayers explains the Poisson like distribution of the fluorescence intensity. According to our multilayer model, the asymmetrical distribution is due to a superimposition of Gaussian's each representing the intensity profile of a distinct number of stacked layers. The amplitude of the Gaussian's decreases with increasing intensity. This can be explained by the assumption that multilayers consisting of $n+2$ layers can only form from those consisting of n layers so that the surface covering decreases with increasing number of layers i. e. increasing fluorescence intensity (see Fig. 8). This would result in the asymmetrical intensity distribution observed. With decreasing area available for the film on compression, the probability of formation of complex multilayer rises leading to a more asymmetric distribution. The mean fluorescence intensity of the collapse phase calculated according to Eq. (4) increases although the relative intensity per dye molecule stays constant.

The described multilayer model has been confirmed by scanning force microscopic (SFM) investigations on

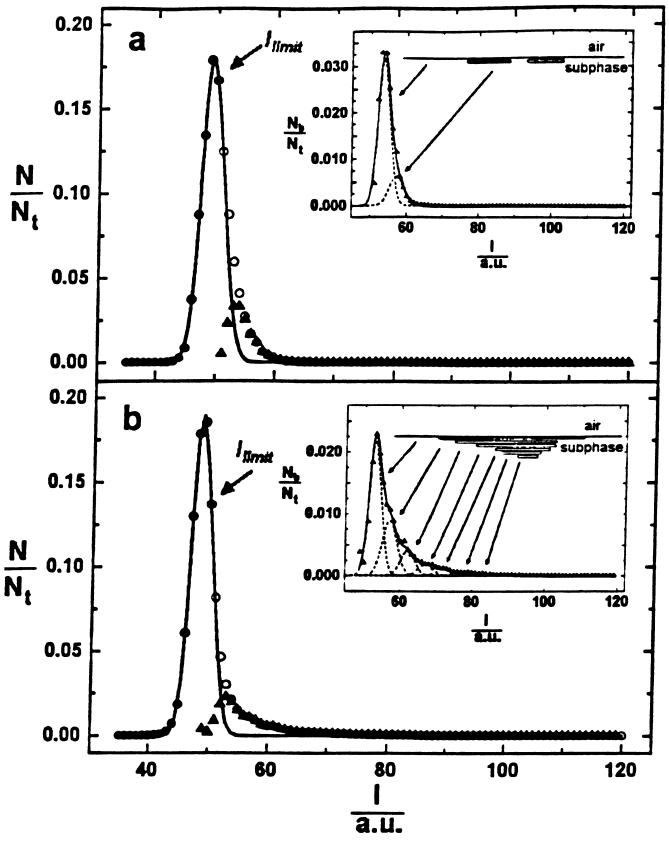

Fig. 8 a, b Histograms evaluated from fluorescence images taken from a lipid/SP-C (DPPC/DPPG/SP-C, lipid molar ratio 4 : 1, protein content 0.4 mole%; dye: NBD-SP-C, 100% of protein) film. Images were taken at the onset (**a**) ($A_M = 0.38$ nm^2) and the end (**b**) ($A_M = 0.27$ nm^2) of the plateau region of the isotherm. *Circles* represent the data evaluated from the images. The lines were calculated by fitting a Gaussian to a part of the intensity distribution of the dark domain (*solid circles*, $I \leq I_{\text{limit}}$). *Triangles* represent the intensity distribution of the bright domain N_b evaluated by subtraction of the Gaussian from the whole distribution N. The *inlets* show the intensity distribution N_b. The *solid lines* were calculated by fitting a sum of Gaussian's to the distribution. The Gaussian's (*dotted lines*) are separated from each other by equidistant intensity steps. The half widths were fixed. According to our model depicted in the upper right part of each diagram, each Gaussian represents the intensity distribution of a distinct number of layers from the multilayer stacks

the collapse structures after LB transfer to a mica support (von Nahmen et al. 1997). Multilayer stacks are clearly visible in the images. The location and the extension of the structures coincides with those found in the fluorescence microscopic images. The step heights evaluated from the SFM images matches the thickness of one lipid bilayer.

From the constant, low fluorescence intensity per dye during compression in the collapse region, we conclude that the lipids are in a condensed, or crystalline like state in the multilayer. Owing to the similarity of the proposed multilayer structures to multilamellar vesicles, this experimental finding is obvious assuming the same level of hydration in both structures: calorimetric investigations on model surfactants in vesicular solution (Perez-Gil et al. 1994; Shiffer et al. 1993) showed that the main phase transition from the gel to the fluid state of the vesicles is shifted to higher temperatures with increasing SP-C content. Even the pure lipid system used in the present study exhibits a phase transition temperature of 42 °C consistent with a gel state of the proposed multilayer structure. From a physiological point of view, a fluid state would be more efficient concerning fast respreading on expansion. For that reason, the high content of unsaturated lipids and cholesterol found in lung lavage may be physiologically important since such additives would lower the phase transition temperature.

The relative area of the bright domain A_b^* remained constant during compression in the collapse region, indicating that the material collecting in the multilayer structures cannot originate solely from the monolayer of the former expanded phase. If that were the case, the relative area of the bright domain would decrease during compression. This indicates that phospholipids of the dark domains must melt in the rim region of the domains. Together with SP-C and other lipids of the bright domain this material contributes to the growing multilayer stacks during compression.

One important fact cannot be explained by the "squeeze out" hypothesis: The material squeezed out has to respread very fast to the air-water interface on inhalation to ensure a total covering of the liquid phase and, therefore, a low surface tension. If the material squeezed out is located in the liquid hypophase, respreading is allowed only by diffusional processes. But, as shown by Oosterlaken-Dijksterhuis et al. (1991), spreading of surfactant in the form of vesicular structures from the subphase takes at least some minutes, i. e. is too slow to ensure a low surface tension during the breathing cycle. The present study shows that upon compression a multilayer structure forms which is in close contact with the monolayer. Such a structure was predicted recently by Schürch et al. (1995), who observed multilayers of surfactant by electron microscopy on thin sections of rabbit lungs. Owing to the fact that these structures may store surfactant material on compression, they called them "surface-associated surfactant reservoir". From our present study there is strong evidence that SP-C enables the formation of this reservoir. This assumption is also supported by the fact that the appearance of the reservoir in the form of multilayer structures fits perfectly with the molecular structure of the protein as pointed out by Amrein et al. (1997).

The present study demonstrates that the hypophase of alveoli contains a minimum of three kinds of surfactant structures: vesicular structures secreted by the epithelial cells, the surface active monolayer, and multilayer structures which are in close contact to the monolayer. Stabilization and reversibility of the multilayer structures can be explained by the presence of SP-C.

Appendix

According to the assumption that all dye molecules are solved in the expanded phase (surface concentration

$\Gamma_{d,dye} \cong 0$), the surface concentration of the dye in the bright domain $\Gamma_{b,dye}$ can be calculated according to

$$\Gamma_{b,dye} = \frac{x_{dye}}{A_b^* \cdot A_M \cdot N_A} \quad \text{(A 1)}$$

where x_{dye} is the mole fraction of dye in the spread mixture, and N_A is Avogadro's number. The denominator represents the area per mole of the surface accessible for the dye.

Since the surface concentration of the dye in the condensed phase is assumed to be negligible, the intensity difference $\overline{\Delta I} = \overline{I_b} - \overline{I_d}$ between the domains is a measure of the fluorescence intensity of the film per area of the size of a pixel. This value is linearly dependent on the fluorescence intensity per dye molecule I_{dye} and the surface concentration of the dye:

$$\overline{\Delta I} = C_{app} \cdot I_{dye} \cdot \Gamma_{b,dye} \cdot N_A \quad \text{(A 2)}$$

where C_{app} is a constant describing the geometrical arrangement of the experiment, the optical properties of the microscope, and the gain of the detection system. Inserting Eq. (A 1) and rearranging, one gets an expression for the fluorescence intensity per dye:

$$I_{dye} = \frac{1}{C_{app} \cdot x_{dye}} A_b^* \cdot A_M \cdot \overline{\Delta I} \quad \text{(A 3)}$$

If the dye molecules are not interacting with each other and are randomly oriented with respect to the surface, I_{dye} is independent of the surface concentration and, therefore, also independent of the molecular area:

$$\lim_{A_M \to \infty} \frac{1}{C_{app} \cdot x_{dye}} \cdot A_b^* \cdot A_M \cdot \overline{\Delta I} = I_{dye}^{\infty} = \text{const} \quad \text{(A 4)}$$

In the case of higher surface concentrations, I_{dye} will decrease because of self-quenching of the dyes. Another reason for a decrease of I_{dye} can be a wrong orientation of the transition moment in respect to the excitation light due to condensation processes in the surface.

On the basis of Eqs. (A 3) and (A 4) one can define a relative fluorescence intensity per dye

$$I_{dye}^* = \frac{I_{dye}}{I_{dye}^{\infty}} \quad \text{(A 5)}$$

which ranges from 0 to 1. I_{dye} cannot be evaluated from measured data because C_{app} is not determinable. In contrast, I_{dye}^* can be easily evaluated from fluorescence microscopic experiments if one measures $\overline{\Delta I}$ over a wide range of molecular areas, and the dye molecules are exclusively solved in the less dense phase using the expression

$$I_{dye}^* = \frac{1}{C \cdot x_{dye}} \cdot A_b^* \cdot A_M \cdot \overline{\Delta I} \quad \text{(A 6)}$$

$C = I_{dye}^{\infty} \cdot C_{app}$ is a constant which can be determined applying Eq. (A 4) at high molecular areas.

Acknowledgements The generous support by Byk-Gulden Pharmaceuticals with the recombinant protein SP-C is gratefully acknowledged. We also thank Dr. Heinrich Luftmann for the help with the mass spectrometric analysis, and Prof. Dr. Richard Wennberg for helpful discussions and careful English corrections.

References

Albrecht O, Gruler H, Sackmann E (1978) Polymorphism of phospholipid monolayers. J Phys (Paris) 39: 301

Amrein M, Nahmen A von, Sieber M (1997) A scanning force- and fluorescence light microscopy study of the structure and function of a model pulmonary surfactant. Eur Biophys J 26: 349–357

Baatz JE, Elledge B, Whitsett JA (1990) Surfactant protein SP-B induces ordering at the surface of model membrane bilayers. Biochemistry 29: 6714–6720

Beers MF, Fisher AB (1992) Surfactant protein C: a review of is unique properties and metabolism. Am J Physiol 263: 151–160

Curstedt T, Jörnvall H, Robertson B, Bergmann T, Berggren P (1987) Two hydrophobic low-molecular-mass protein fractions of pulmonary surfactant: characterization and physical properties. Eur J Bioch 168: 255–262

Harwood JL (1987) Lung surfactant. Prog Lipid Res 26: 211–256

Horowitz AD, Elledge B, Whitsett JA, Baatz JE (1992) Effects of lung surfactant proteolipid SP-C on the organization of model membrane lipids: a fluorescence study. Biochim Biophys Acta 1107: 44–54

Johansson J, Curstedt T, Robertson B (1994 a) The proteins of the surfactant system. Eur Respir J 7: 372–391

Johansson J, Szyperski T, Wüthrich K (1995) Pulmonary surfactant-associated polypeptide SP-C in lipid micelles: CD studies of intact SP-C and NMR secondary structure determination of depalmitoyl-SP-C (1–17). FEBS Lett 362: 261–265

Johansson J, Szyperski T, Curstedt T, Wüthrich K (1994 b) The NMR structure of the pulmonary surfactant-associated polypeptide SP-C in an apolar solvent contains a valyl-rich α-helix. Biochemistry 33: 6015–6023

King RJ, Clements JA (1972) Surface active material from dog lung. I. Method of isolation. Am J Physiol 223: 715–726

Leufgen KM, Rulle H, Benninghoven A, Sieber M, Galla H-J (1995) Imaging time-of-flight secondary ion mass spectrometry allows visualization and analysis of coexisting phases in Langmuir-Blodgett films. Langmuir 12: 1708–1711

Lösche M, Möhwald H (1984) A fluorescence microscope to observe dynamical processes in monomolecular layers at the air/water interface. Rev Sci Instrum 55: 1968–1972

McConnel HM, Tamm LK, Weiss RM (1984) Periodic structures in lipid monolayer phase transitions. Proc Natl Acad Sci USA 81: 3249–3253

Miyano H, Toyo'oka T, Imai K (1985) Further studys on the reaction of amines and proteins with 4-fluoro-7-nitrobenzo-2-oxa-1,3-diazole. Anal Chim Acta 170: 81–87

Nag K, Bolan C, Rich N, Keough KMW (1991) Epifluorescence microscopic observation of monolayers of dipalmitoylphosphatidylcholine: dependence of domain size on compression rates. Biochim Biophys Acta 1068: 157–160

Nag K, Rich N, Keough KMW (1994) Interaction between dipalmitoylphosphatidylgylcerol and phosphatidylcholine and calcium. Thin Solid Films 244: 841–844

Nag K, Perez-Gil J, Cruz A, Keough KMW (1996) Fluorescently labeled pulmonary surfactant protein C in spread phospholipid monolayers. Biophys J 71: 246–256

Nahmen A von, Schenk M, Sieber M, Amrein M (1997) The structure of a model pulmonary surfactant as revealed by scanning force microscopy. Biophys J 72: 463–469

Nichols JW, Pagano RE (1981) Kinetics of soluble lipid monomer diffusion between vesicles. Biochemistry 20: 2783–2789

Oosterlaken-Dijksterhuis MA, Haagsman HP, van Golde LMG, Demel RA (1991) Interaction of lipid vesicles with monomolecular layers containing lung surfactant proteins SP-B or SP-C. Biochemistry 30: 8276–8281

Perez-Gil J, Nag K, Taneva S, Keough KMW (1992) Pulmonary surfactant protein SP-C causes packing rearrangements of dipalmitoylphosphatidylcholine in spread monolayers. Biophys J 63: 197–204

Perez-Gil J, Lopez-Lacomba JL, Cruz A, Beldarrain A, Casals C (1994) Interfacial adsorption of simple lipid mixtures combined with hydrophobic surfactant protein from pig lung. Biochem Soc Trans 22: 22

Post A, Nahmen A von, Schmitt M, Ruths J, Riegler H, Sieber M, Galla H-J (1995) Pulmonary surfactant protein C containing lipid films at the air-water interface as a model for the surface of lung alveoli. Mol Membr Biol 12: 93–99

Scarpelli EM, Mautone AJ (1994) Surface biophysics of the surface monolayer theory is incompatible with regional lung function. Biophys J 67: 1080–1089

Schürch S, Qanbar R, Bachofen H, Possmayer F (1995) The Surface-Associated Surfactant Reservoir in the Alveolar Lining. Biol Neonate 67: 61–76

Shiffer K, Hawgood S, Haagsman HP, Benson B, Clements JA, Goerke J (1993) Lung surfactant proteins, SP-B and SP-C, alter the thermodynamic properties of phospholipid membranes: a differential calorimetry study. Biochemistry 32: 590–597

Taneva SG, Keough KMW (1994 a) Dynamic surface properties of pulmonary surfactant proteins SP-B and SP-C and their mixtures with dipalmitoylphosphatidylcholine. Biochemistry 33: 14660–14670

Taneva SG, Keough KMW (1994 b) Pulmonary surfactant proteins SP-B and SP-C in spread monolayers at the air-water interface: I. Monolayers of pulmonary surfactant protein SP-B and phospholipids. Biophys J 66: 1137–1148

Taneva SG, Keough KMW (1994 c) Pulmonary surfactant proteins SP-B and SP-C in spread monolayers at the air-water interface: II. Monolayers of pulmonary surfactant protein SP-C and phospholipids. Biophys J 66: 1149–1157

Taneva SG, Keough KMW (1994 d) Pulmonary surfactant proteins SP-B and SP-C in spread monolayers at the air-water interface: III. Proteins SP-B plus SP-C with phospholipids in spread monolayers. Biophys J 66: 1158–1166

Toyo'oka T, Watanabe Y, Imai K (1983) Reaction of amines of biological importance with 4-fluoro-7-nitrobenzo-2-oxa-1,3-diazole. Anal Chim Acta 148: 305–312

Wang Z, Hall SB, Notter RH (1995) Dynamic surface activity of films of lung surfactant phospholipids, hydrophobic proteins, and neutral lipids. J Lipid Res 36: 1283–1293

Watkins JC (1968) The surface properties of pure phospholipids in relation to those of lung extracts. Biochim Biophys Acta 152: 293–306